# RSC Advances

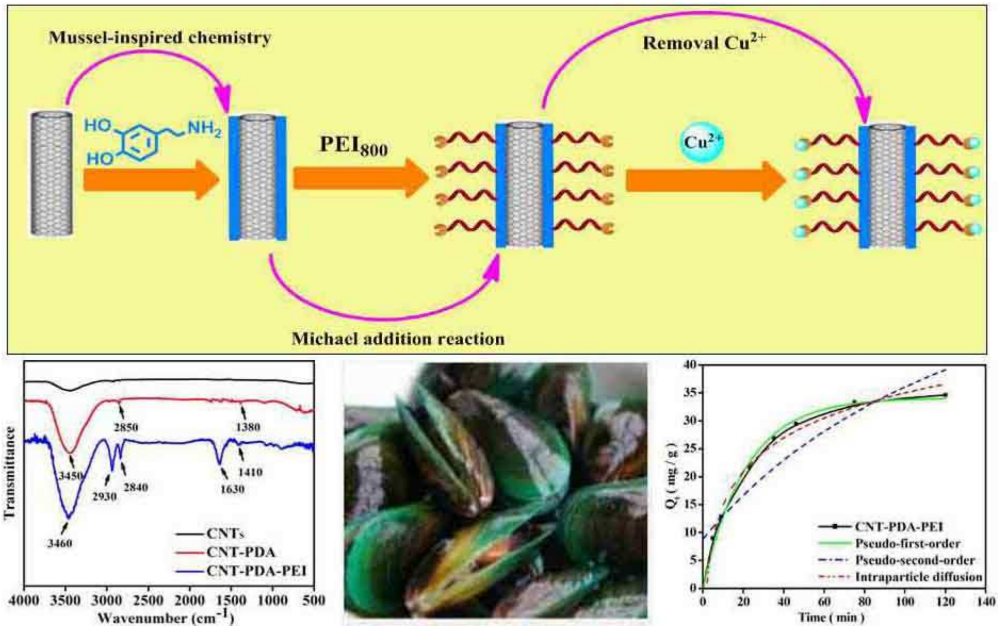

Polyethylenimine functionalized carbon nanotubes were prepared through mussel inspired chemistry and Michael addition reaction and utilized for adsorption of $Cu^{2+}$ from water.

RSC Advances

Cite this: DOI: 10.1039/c0xx00000x

www.rsc.org/xxxxxx

Full Paper

# Mussel Inspired Functionalization of Carbon Nanotubes for Heavy Metal Ion Removal

**Yili Xie[a], Qiang Huang[b], Meiying Liu[b], Ke Wang[c], Qing Wan[b], Fengjie Deng[b], Long Lu[a,*], Xiaoyong Zhang[b,*], Yen Wei[c,*]**

***Received (in XXX, XXX) Xth XXXXXXXXX 200X, Accepted Xth XXXXXXXXX 200X***

**DOI: 10.1039/b000000x**

Carbon nanotubes (CNTs) have been widely used as adsorbents to remove various environmental pollutants because of their unique one dimensional structure, large surface areas and amounts of micropores. However, the adsorption capacity of unmodified CNTs toward heavy metal ions is still limited due to their poor dispersibility and lack of functional groups. In this work, a novel strategy has been developed to prepare polyethylenimine functionalized CNTs via combination of mussel inspired chemistry and Michael addition reaction. The successful preparation of CNTs with amine groups was confirmed by a series of characterized measurements such as transmission electron microscopy, fourier transform infrared spectroscopy, thermal gravimetric analysis. Furthermore, the adsorption application of these amine functionalized CNTs toward $Cu^{2+}$ was also examined. Various factors included contact time, pH values, temperature and initial $Cu^{2+}$ concentrations on the adsorption capability of amine functionalized CNTs were also investigated. Langmuir and Freundlich models were used for thermomechanical analysis. The pseudo-first-order, pseudo-second-order and intra-particle diffusion model were used for the kinetic analysis. Results demonstrated that CNTs can be successfully functionalized with amine groups through a rather facile and mild bioinspired strategy. And these amine functionalized CNTs exhibited much enhanced adsorption effeciency toward $Cu^{2+}$. Given the strong and versatile adhesion of PDA to various materials, the bioinspired strategy described in this work could also be utilized for fabrication of many other nanocomposites for environmental applications.

## 1. Introduction

Under the current circumstance, human beings pay much attention to the environmental contaminations, certainly including water pollution.[1] Heavy metal ions, which exist in various industrial waste water, attracting growing attention due to their high toxic, non-biocompatible and easily accumulate in living organisms.[2-7] Among them, copper ion (label as $Cu^{2+}$), was considered to be one of the most poisonous ions, normally dissolved into wastewater and then released into the environment. Though as a significant trace nutrient for the health of human body, when consumed in large dose for a long period may lead to vomiting, cramps, skin rash or even death.[8, 9] As we all know, large amounts of $Cu^{2+}$ were produced in the fields of smelting, metal processing, machinery manufacturing, organic synthesis and other industrial wastewater.[10, 11] Among them, the metal processing, electroplating factories discharge waste water containing copper content is the highest, which has caused serious impacts for living organisms. Therefore removal of $Cu^{2+}$ from wastewater is necessary and urgent.

Due to the villainous consequence of high concentration of $Cu^{2+}$ for human life, in order to resolve these problems, a lot of high-efficiency methods for removal of $Cu^{2+}$ from wastewater have been reported including ion exchange, chemical precipitation, ultrafiltration, reverse osmosis, adsorption and electrodialysis *etc.*[12-17] Among these techniques, the typical strategy of adsorption shows excellently prominent and draws much attention for its high efficiency, simple operation and low cost. On the other hand, with the development of nanotechnology, a large number of nanomaterials, especially carbonaceous nanomaterials (e.g. carbon nanotubes (CNTs), graphene oxide), are used as adsorbent because of their broad pore volume, large specific surface area and stable covalent chemical bonds.[18, 19] CNTs, a class of popular carbon nanomaterials, have been widely applied in the various fields such as drug delivery, machine manufacturing, environmental protection and so on because of their great mechanical properties, high chemical stability, unique electronic properties and diameter ratio.[20] Recently, accompanying with in-depth research for the CNTs, the excellent performances of huge specific surface areas and loose structure of CNTs have attracted much attention in adsorption field, which could serve as high-efficiency agents to remove other heavy ions.[21-31] Although these perfect performances they possess, unfortunately, poor dispersibility and lack of functional groups inevitably restricted adsorption capacity of CNTs toward heavy metal ions. In recent years, many strategies for the surface modification of CNTs to enhance their dispersibility in aqueous solution have been developed.[32-39] However, the commonly adopted noncovalent and covalent strategies still have some drawbacks, which include the instability of noncovalent methods, and low effeciency, complexicity and time consuming of covalent strategy. Therefore, the development of facile surface modification strategies for preparation of CNTs with good adsorption performance is still high desirable.

As a versatile surface modification strategy, mussel-inspired chemistry has attracted increasing attention for wide applications ranged from biological imaging and cancer treatment to energy conversion and environmental protection.[40-57] Since being discovered of this novel strategy by Lee in 2007, mussel-inspired chemistry has become versatile and facile surface modification method to any materials included metal and non-metal materials regardless of their composition, shape and size because of strong and universal adhesive of polydopamine (PDA), which was formed via self-oxidation of dopamine in alkaline solution. Furthermore, after coating PDA coating to the material surface, many reactive sites were introduced to the surface of material, which can further be covalently conjugated with amino- or thiol-contained molecules.[43] For example, our previous work had reported that surface modification of CNTs with thiol-contained small organic molecules and amino-terminated polymer to increase the dispersibility of CNTs materials via combination of mussel-inspired chemistry and Michael addition reaction. These functional CNTs suggest obviously enhanced dispersion in aqueous and some organic solutions.[58-61] Polyethylenimine (PEI), as abundant amino groups organic hydrophilic molecules, have been wildly used in surface modification of adsorbents due to its luxuriant amine groups including primary, secondary and tertiary amines which exhibits perfect adsorption ability for heavy metals.[62] Therefore, inspired by this facile surface functional methods, amine functionalized CNTs can be prepared through the Michael addition reaction between PDA and PEI.

In this work, stiff CNT surface was perfectly modified with hydrophilic PEI to endow their excellent dispersibility in water and absorbility toward $Cu^{2+}$ via combination of mussel-inspired chemistry and Michael addition reaction. The specific procedure was shown in **Scheme 1**: two mild steps were involved in the process for preparation of functionalized adsorbents. First, the PDA coating was formed on the surface of CNTs in aqueous solution (pH = 8.5) via mussel inspired chemistry. Afterwards, PEI molecules were efficiently conjugated onto the surface of functional CNT with PDA through Michael addition reaction. Finally, the obtained amine functionalized CNTs were applied to remove $Cu^{2+}$. The influencing impacts for removing $Cu^{2+}$ include pH, contact time, temperature and initial $Cu^{2+}$ concentration were investigated in this work.

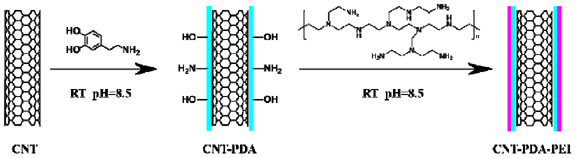

**Scheme 1** Schematic representation for the preparation of CNTs-PDA-PEI via the combination of mussel-inspired chemistry and the Michael addition reaction.

## 2. Experiment

### 2.1 Materials

CNTs from the nanopowder Co. were synthesized by chemical vapor deposition. The diameter of CNTs is about 30-50 nm according to the manufacturer. The dopamine hydrochloride was purchased from Sangon Co. Tris-(chydroxymethyl)-aminethane (Tris) (>99%) was obtained from Tianjin Heowns Biochem.LLC.Co. PEI (molecular weight 800 Da) and copper nitrate trihydrate (> 99.99%) were purchased from Aladdin Industrial Co. Deionized water was prepared for the usage of solution.

### 2.2 Characterization

The morphology of modified CNT-PDA-PEI adsorbent was ensured by transmission electron microscopy (TEM). The TEM images were supplied from a Hitachi 7650B microscope operated at 80 kV by using a little glob of nanoparticle ethanol suspension on a carbon-coated copper grid as the TEM specimens. Fourier transform infrared spectroscopy (FT-IR) is used to confirm the structure composition and chemical functional groups of modified CNT-PDA-PEI. The Fourier transform infrared (FT-IR) spectra were obtained from Nicolet5700 (Thermo Nicolet corporation). Thermal gravimetric analysis (TGA), which was conducted on a TA instrument Q50 with a heating rate of 20 °C $min^{-1}$ is bring for determination of the thermal properties of modification of CNT-PDA-PEI under air atmosphere.

### 2.3 Synthesis of CNT-PDA

The synthesis method of CNT-PDA nanocomposites is in detail as follows: 1 g of CNTs and 1 g of dopamine hydrochloride were simultaneously added into a 500 mL flask with Tris buffer solution (pH = 8.5, 10 mM) into the flask to make 250 mL solution. After that, the suspensions were treated with ultrasonator for about 5 min and magnetic stirred for 8 h. Finally centrifuged under 8000 rpm for 10 min, washed for 3 times with deionized water and dried at 323 K for 24 h.

### 2.4 CNT-PDA-PEI

The CNTs-PDA-PEI was synthesized by the same method mentioned above. 1 g of PEI and 1 g of CNTs-PDA were added into a 500 mL flask using deionized water with Tris buffer solution, then ultrasonator for 5 min and stirred for 8 h, centrifuged, washed with pure water three times and dried at vacuum for further adsorption experiment.

### 2.5 Absorbed capacity of CNT-PDA-PEI for $Cu^{2+}$

Batch adsorption experiments were used to study the removal of $Cu^{2+}$ under the impact of the following parameters: contact temperature, pH value, contact time and the initial $Cu^{2+}$ concentration. In general, 10 mg adsorbent was added into 50 ml of the $Cu^{2+}$ solution (10 mg/L) in the 50 mL sample tube. The equilibrium $Cu^{2+}$ concentration were determined by the ultraviolet and visible spectrophotometer. The effect of contact temperature studied at different temperatures (303, 313, 323, 333, 343, 353 K) with the same amount of the adsorbent and the $Cu^{2+}$ concentration. The effect of pH experiment studied by change the $Cu^{2+}$ concentration pH from 2 to 10 by adding 0.1 M HCl and 0.1 M NaOH solutions. The influence of $Cu^{2+}$ concentration experiment tested by different initial $Cu^{2+}$ concentration in the range of 10 mg/L to 120 mg/L The final adsorption capacity (***Qe***, mg/g ) and the $Cu^{2+}$ removal efficiency ( R % ) were analyzed by the following equation, respectively:

$$Q_e = \frac{(C_0 - C_t)V}{m}$$

$$R = \frac{100(C_0 - C_t)}{C_0}$$

Where V (mL) is the $Cu^{2+}$ solution volume, m (mg) is the adsorbent dose, $C_0$ (mg/L) is the $Cu^{2+}$ initial concentration and $C_t$ is the equilibrium $Cu^{2+}$ concentration. ***Qe*** (mg/g) is the adsorption capacity at the equilibrium time. And R (%) is the removal efficiency of the $Cu^{2+}$ solution.

## 3. Results and discussion

### 3.1 Characterizations of CNTs nanocomposites

The surface modification CNTs with abundant amino group organic molecule (PEI) were prepared via a novel strategy of mussel-inspired chemistry and Michael addition reaction. The TEM images of CNTs sample could demonstrate that PDA coating and PEI were perfectly covered on the surface of CNTs. As we can see from the **Fig. 1A**, the diameter of pristine CNTs was about 30 to 50 nm, which was consistent with information provided from manufacturers. And the surface of pristine CNTs is especially smooth from the observation of **Fig. 1A**. After modifying with PDA on the CNT surface via mussel-inspired chemistry, as shown in the Fig. S1, the CNT surface change into slight coarse from the smooth surface, which provide direct evidence that successful modification of CNT surface with PDA coating as well. These results could successfully demonstrate that strong adhesion of PDA is efficient to inorganic materials. The phenomenon of **Fig. S1** could illustrate that mussel-inspired chemistry is suitable to any materials. After PEI molecules were covalently conjugated onto the CNT-PDA surface via typical Michael addition reaction. Blurry coating on the CNT surface can be observed (as marked with red arrows in **Fig 1B** and **Fig. S2**). Based on the enlarged TEM image of CNT-PDA-PEI, the thinkness of PDA coating is about 8 ± 1 nm. These results evidenced that PEI was grafted onto the surface of CNTs due to the role of Michael addition reaction. From the analysis of TEM, we concluded that successful modification of CNTs with hydrophilic PEI to enhance their dispersion via combination of mussel inspired chemistry and Michael addition reaction. More importantly, the novel strategy described in this work is also suitable other materials to endow their excellent properties.

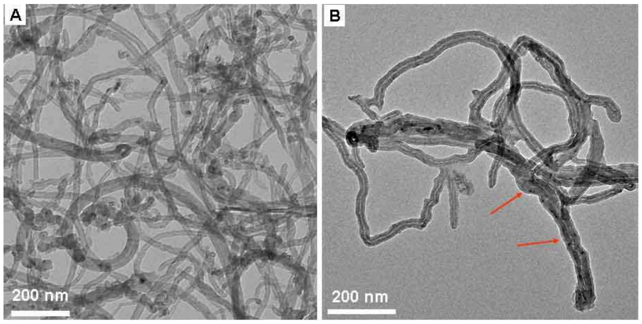

**Fig. 1** The representative TEM images of CNTs samples. (A) pristine CNTs, (B) CNT-PDA-PEI. Which primarily demonstrate that successful modification of CNTs with PDA and PEI via combination of mussel-inspired chemistry and Michael addition reaction.

Exception of high-resolution TEM characterized technique, the representative FT-IR technique were also employed to determine whether the surface of CNTs are successfully modified using PDA and PEI as templets. As shown in **Fig 2A**, although there were no particular peaks could be observed from pristine CNTs, after PDA was coated on the CNT surface because of their strong adhesion to any materials, the characterized peak located at 3450 $cm^{-1}$ was observed, which attributed to the stretching vibration of $-NH_2$ bonds. On the other hand, the characterized peak appeared at 2850 $cm^{-1}$ could be ascribed to the stretching vibration of $–CH_2$ existed in the catechol. These results demonstrated that PDA coating is surely formed on the CNT surface by facile mussel-inspired chemistry surface modification method. Based on the typical Michael addition reaction, the PEI molecules could be facilely conjugated onto the surface of CNT-PDA, the powerful evidence which could be used to verify the successful conjugation of PEI to the CNT-PDA surface is that new peak appeared at 2930 $cm^{-1}$ of $–CH_3$ bonds. Furthermore, the two characterized peaks respectively located at 1630 and 1410 $cm^{-1}$ could be ascribed to the vibration of C-N (simple harmonic vibration) and C-C (flexible vibration) bonds. Therefore, the FT-IR specta for CNT samples demonstrated that functional CNTs using PEI were prepared based on mussel-inspired chemistry and Michael addition reaction.

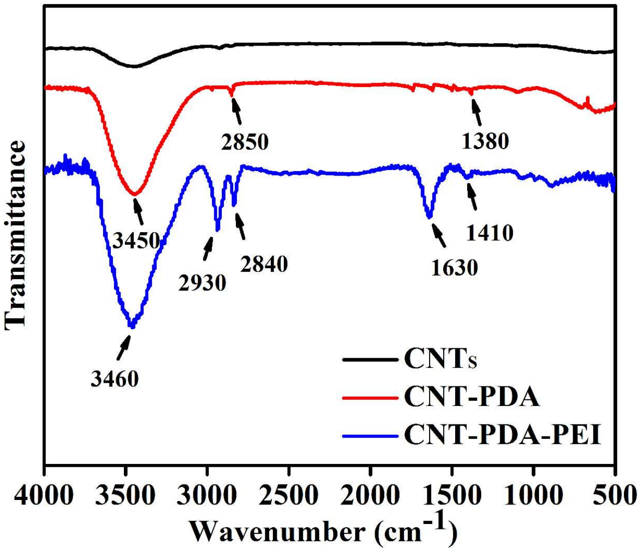

**Fig. 2** FT-IR spectra for CNTs, CNT-PDA, CNT-PDA-PEI nanoparticles.

The relative content of PDA and PEI conjugated onto the surface of CNTs could be confirmed by TGA measurement. As we can see from the TGA curves of CNT samples (**Fig. S3**), the weight loss of pristine CNTs was approximately 1.17% when the temperature ascended from 100 to 500 °C under nitrogen atmosphere. The slight weight loss of pristine CNTs under high temperature suggested that CNTs possess excellent thermal stability. On the other hand, the pronounced drop of weight loss for the CNT samples (weight loss: 19.30%) could also be observed in the **Fig. S3** when temperature raised from 500 to 600 °C, suggesting that the decomposition temperature of CNTs is 500 °C. However, after formation of PDA on the CNT surface due to the self-polymerization of DA in the alkaline solution, the weight loss arrived to 9.81% when temperature was increased from 100 to 500 °C. Compared to the pristine CNTs, the change of weight loss of CNT-PDA under the same temperature could be explained that the oxygen content was enhanced because of the introduction of PDA coating on the CNT surface, which evidenced that successful formation of PDA coating on the CNT surface by mussel-inspired chemistry. The content of PDA coating on the CNT surface could be calculated as 8.64%. After adding the PEI to the surface of CNT-PDA via Michael addition reaction, the weight loss of CNT-PDA-PEI samples was increased to 40.1% in air atmosphere (**Fig. S3**). Compared with CNT-PDA, the weight loss of CNT-PDA-PEI was significantly increased from 19.3 to 40.1%, further demonstrated that PEI was successfully conjugated onto CNT-PDA surface via typical Michael addition reaction.

### 3.2 Adsorption experiment studies

#### 3.2.1 Effect of contact time and adsorption kinetics

The effect of contact time on $Cu^{2+}$ removal by the pristine CNTs and CNT-PDA-PEI is shown in below **Fig. 3**. Obviously, the modified CNT-PDA-PEI nanocomposites show better adsorption performance than pristine CNTs, which demonstrated that PEI molecules were covalently conjugated onto the surface of CNT-PDA via typical Michael addition reaction. The $Cu^{2+}$ equilibrium adsorption capacity of CNTs is just 25.4 mg/g while $Q_t$ of the CNT-PDA-PEI reach up to 34.6 mg/g by a large margin which is due to the abundant amine groups existed in PEI macromolecules on the surface of CNTs. Therefore the dramatic improvement of the adsorption capacity also suggested the perfect prosperity of adsorption of CNTs modified with PEI for $Cu^{2+}$ removal. More importantly, the obvious enhancement of absorption of CNT-PDA-PEI than CNTs materials provides direct evidence that feasibility of this novel strategy described in this work for surface modification of materials. The above results suggested that the amine groups on the adsorbent (CNT-PDA-PEI) play an important role for the enhancement of adsorption capacity, indicating that novel adsorption mechanism was invovled in the adsorption procedure of CNT-PDA-PEI. It is well known that introduction of functional groups such as carboxyl groups and amino groups on CNTs can improve the adsorption capability of these adsorbents through increasing the active adsorption sites.[63] These adsorption of enhancement is mainly due to the coordination of functional groups with cation ions. Most of these interaction is not a specific interaction. Therefore, the CNT-PDA-PEI are not selective adsorbents toward $Cu^{2+}$.

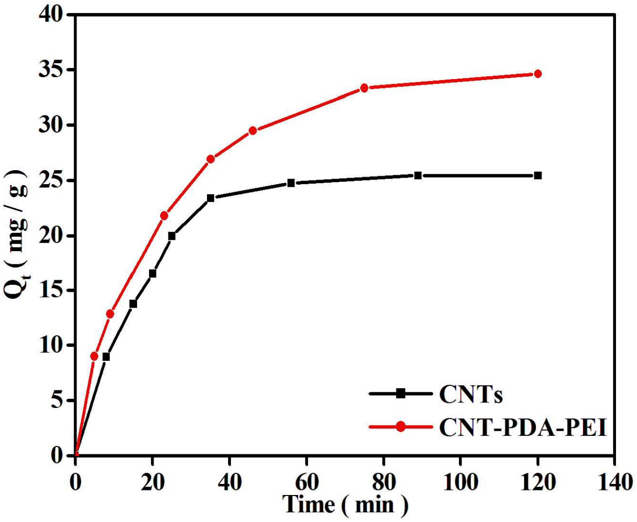

**Fig. 3** The effect of contact time to $Cu^{2+}$ adsorption with the initial $Cu^{2+}$ concentrations of 10 mg/L at room temperature.

The non-linear form of the pseudo-first-order kinetic model is given as follows:

$$Q_t = Q_e(1 - e^{-k_1 t})$$

Where $Q_t$ (mg/g) is the quantity of $Cu^{2+}$ adsorbed by CNT-PDA-PEI at different contact time t (min), $Q_e$ (mg/g) is the equilibrium adsorption capacity, $K_1$ ($min^{-1}$) is the pseudo-first-order equation rate constant. The values of these parameters and $K_1$, correlation coefficient ($R^2$) are listed in **Table 1**. The following equation often used to describe the non-linear form of the pseudo-second-order kinetic model.

$$Q_t = \frac{k_2 Q_e^2 t}{1 + k_2 Q_e t}$$

$$h = k_2 Q_e^2$$

Where $Q_e$ (mg/g) and $Q_t$ (mg/g) are the adsorption capacity of modified adsorbent CNT-PDA-PEI at equilibrium and different time t (min), respectively. $K_2$ (g. $mg^{-1}$.$min^{-1}$) is the rate constant of the pseudo-second-order, $h$ (mg/g.min) is the initial adsorption rate of the $Cu^{2+}$ removal process. All the parameters and $R^2$ are also listed in **Table 1**. This study brings in intra-particle diffusion model to further test the reaction rate of adsorption process. And it can be described by the equation as follows:

$$Q_t = k_p t^{0.5}$$

Where $Q_t$ (mg/g) is the adsorption capacity under any time t (min) as the above described, $K_p$ ($mg \cdot g^{-1} \cdot min^{-1/2}$) is the rate constant of the intra-particle diffusion model. The value of $K_p$ (mg $g^{-1}$ $min^{-1/2}$) and $R^2$ are listed in **Table 1**. According to the results summarized in **Table 1,** the correlated coefficient ($R^2$) from pseudo-first-order is 0.994, which is much higher than the correlation coefficient (***$R^2$*** = 0.841) from pseudo-second-order. These results indicated that the adsorption kinetic better followed the pseudo-first-order kinetic model. However the intra-particle diffusion is the rate-controlling step of the adsorption process due to the relatively high correlation coefficient (***$R^2$*** = 0.985) from intra-particle diffusion kinetic model. In summary, several steps happened in the adsorption process could be classified as follows: the instantaneous step occurred at first on the apparent surface, gradual adsorption step happened as the rate-controlling reaction process. The last equilibrium step with low adsorption efficiency could be attributed to the decrease of the monolayer site and the reduction of $Cu^{2+}$ concentration. As is known to all, the hydrolysis capacity of the $Cu^{2+}$ ion and the competitive adsorption of coexisting matters in aqueous solution both are the influence factors of the $Cu^{2+}$ removal capacity on new composite adsorbent CNT-PDA-PEI. Furthermore, the chemical and physical properties of the chosen adsorbent also have impact on the adsorption process. And incidentally the high adsorption rate in this study may owing to the chemisorption. Therefore, the complexation chemical reaction is expected in the adsorption.

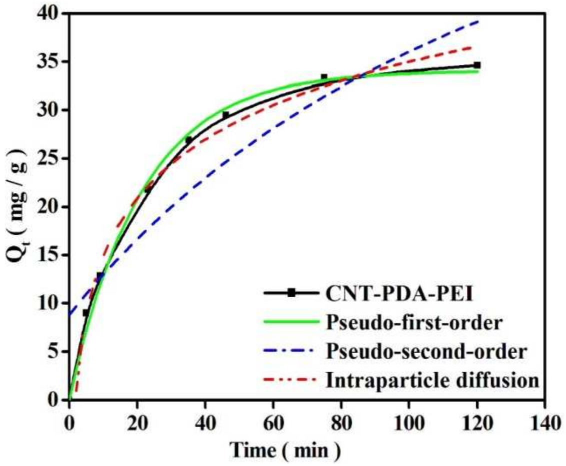

**Fig. 4** Different kinds of adsorption kinetics of CNT-PDA-PEI. The value of data fitted by Pseudo-first-order, Pseudo-second-order and Intra-particle diffusion models, respectively. Experiment proceed at room temperature, pH = 7.0 and 10 mg/L of initial $Cu^{2+}$ concentrations.

**Table 1** adsorption kinetics data of Pseudo-first-order, Pseudo-second-order and Intra-particle diffusion model for $Cu^{2+}$ adsorption on CNT-PDA-PEI.

| Models | Parameters | Initial concentration(mg/L) |
|---|---|---|
| | | 10 |
| Pseudo-first-order | ***$Q_e$*** (cal) (mg/g) | 34.1 |
| | ***$K_2$*** ($min^{-1}$) | 0.0473 |
| | ***$R^2$*** | 0.994 |
| Pseudo-second-order | ***$Q_e$*** (cal) (mg/g) | 79.1 |
| | ***$K_2$*** ($g{\cdot}mg^{-1}{\cdot}ming^{-1}$) | 0.0000799 |
| | ***h*** ($mg{\cdot}g^{-1}{\cdot}ming^{-1}$) | 0.500 |
| | ***$R^2$*** | 0.841 |
| Intra-particle diffusion | ***Kp*** ($mg{\cdot}g^{-1}{\cdot}min^{-1/2}$) | 549797 |
| | ***$R^2$*** | 0.985 |

### 3.2.2 Effect of temperature and thermodynamic study

Temperature is one of indispensable factors in adsorption experiments. The effect of temperature on the removal of $Cu^{2+}$ based on CNT-PDA-PEI was tested at different temperature ranging from 303 to 353 K with the other conditions unchanged. The thermodynamic parameters containing enthalpy change (Δ***$H^0$***), Gibbs free energy (Δ***$G^0$***) and entropy change (Δ***$S^0$***) were determined by using the equations as follows:

$$\ln K\alpha = \frac{\Delta S^0}{R} - \frac{\Delta H^0}{R \cdot T}$$

$$K\alpha = \frac{Q_e}{C_e}$$

$$\Delta G^0 = -RT\ln K\alpha$$

Where ***kα*** is the thermodynamic equilibrium constant, R is represent the gas constant (8.314 J/molK), T is the solution temperature (K). The plot of lnkα as the function of 1/T, Δ***$H^0$*** and Δ***$S^0$*** were calculated from the slope and intercept from the Van't Hoff plots of lnkα with 1/T, respectively. The obtained thermodynamic parameters recorded on **Table 2**. As shown in **Fig 5**, the $Cu^{2+}$ adsorption capacity from 21.6 to 41.0 mg/g which increased clearly with the increase of temperature from 303 to 353 K. In addition, the thermodynamic parameters calculated from above can be seen from **Table 2**, the positive values of Δ***$H^0$*** and the increasing trend of the adsorption capacity with the temperature increase both signified that adsorption process using CNT-PDA-PEI is an endothermic process. And the negative values of Δ***$G^0$*** signified the spontaneous process in nature of the

$Cu^{2+}$ adsorption on CNT-PDA-PEI.

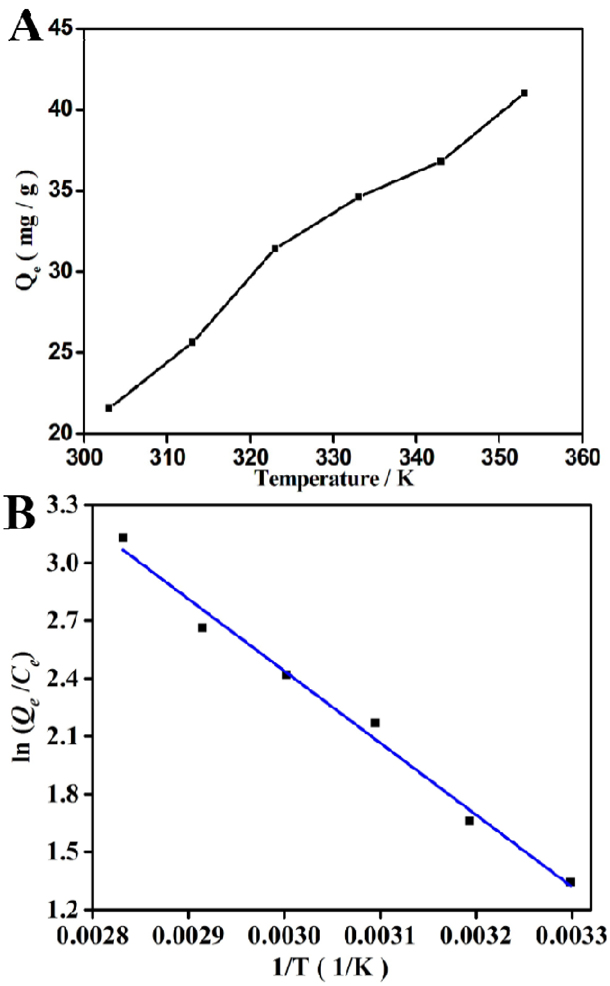

**Fig. 5** (A) The effect of temperature for $Cu^{2+}$ removal on CNT-PDA-PEI. (B) Van't Hoff plot for the $Cu^{2+}$ adsorption process.

**Table 2** Data of the thermodynamic parameters for the adsorption of $Cu^{2+}$ onto CNTs-PDA-PEI nanocomposites

| T (K) | ΔG0 (KJ/mol·K) | ΔH0 (KJ/mol·K) | ΔS0 (KJ/mol·K) |
|---|---|---|---|
| 303 | -3.38 | 34.4 | 0.113 |
| 313 | -4.32 | 35.5 | |
| 323 | -5.85 | 36.6 | |
| 333 | -6.70 | 37.8 | |
| 343 | -7.60 | 38.9 | |
| 353 | -9.18 | 40.0 | |

### 3.2.3 Effect of pH

The influence factor pH gets great value reflect both on the conversion of metal ions from aqueous solution and the protonation degree of amine groups on CNT-PDA-PEI. In order to test the effect of initial pH of $Cu^{2+}$ solution on the adsorption of CNT-PDA-PEI, this work made different initial pH solution at the range of 3 to 12 at room temperature. According to **Fig 6**, the absorption capacity was increased from 4.50 to 47.4 mg/g as the pH was increased from 3 to 10, and then kept stable approximately at pH > 10. For the first rising stage, low adsorption capacity due to the protonation of amine groups on the CNT-PDA-PEI in acidic solutions, however the increased adsorption capacity because of the weakening amine groups to be deprotonated with pH increasing. Gradually in alkaline environment, on account of the porous structure and abundant –$NH_2$ groups with deprotonation on the surface of CNT-PDA-PEI, the adsorption capacity were much considerable, as well as the better coordinate ability between the adsorbent and $Cu^{2+}$. On the other hand, however, part of PDA structure can be damaged in super alkaline environment especially when pH >11 that may hinder the improvement of adsorption capacity and remain the same capacity approximately. As for the removal efficiency in **Fig 6**, an obvious enhancement from 9.09 to 95.7%, which further indicated that the modified CNT-PDA-PEI adsorbent show the great ability of $Cu^{2+}$ removal.

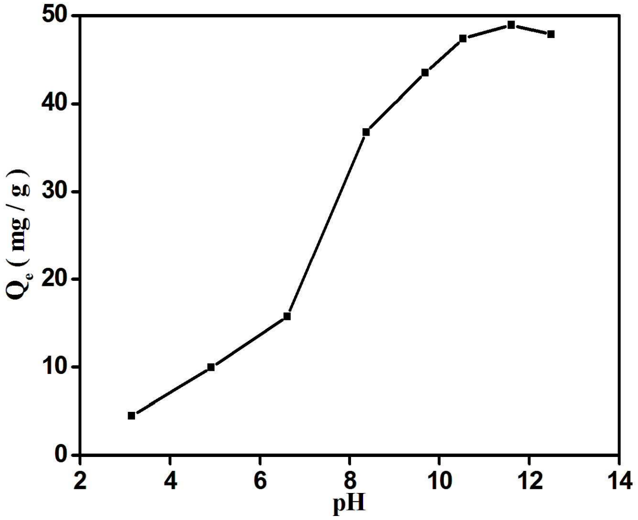

**Fig. 6** The effect of pH of $Cu^{2+}$ removal on CNT-PDA-PEI with 10 mg/L initial $Cu^{2+}$ concentration at room temperature.

### 3.2.4 Adsorption isotherms

Adsorption isotherm manifested the way that adsorbents interact with heavy metal ions or other adsorbates, and also described the adsorption capacity, adsorption strength and the adsorption status. In this work, two significant adsorption isotherm models contained Langmuir and Freundlich isotherms were recommended to analyze the results of the equilibrium isotherms of $Cu^{2+}$ solution used CNT-PDA-PEI as adsorbents under different initial $Cu^{2+}$ concentrations at neutral environment and room temperature.

The Langmuir isotherm also be called the adsorption model of monomolecular layer, just as the name implies the isotherm is based on the assumption that each adsorption site distribute homogeneously on the surface of solid materials and can only adsorb single molecule. The adsorption models can be expressed by the following equation:

$$Q_e = \frac{bQ_mC_e}{1 + bC_e}$$

Where $\boldsymbol{Q_m}$ (mg/g) is the maximum amount of adsorbate during the whole adsorption process, $\boldsymbol{Q_e}$ (mg/g) is the adsorption capacity at adsorption equilibrium, $\boldsymbol{C_e}$ (mg/L) is the equilibrium adsorption amount of adsorbed $Cu^{2+}$ concentration solution, $\boldsymbol{b}$

(l/mg) is the adsorption index and the stronger the ***b*** value, the greater the adsorption process.

The Freundlich isotherm model which is an empirical isothermal equation based on experimental results, which is used to describe the heterogeneous systems and the form of Freundlich equation can be represented as follows:

$$Q_e = K_F C_e^{\frac{1}{n}}$$

Where $\boldsymbol{Q_e}$ (mg/g) is the equilibrium adsorption capacity, $\boldsymbol{C_e}$ (mg/L) is the equilibrium $Cu^{2+}$ concentration solution, $\boldsymbol{K_F}$ [(mg/g) (l/mg)$^{1/n}$] is an correlation index reflected to the adsorption capacity, ***n*** is the adsorption constant as well to indicate the adsorption intensity. The above adsorption isotherm parameters and the correlation coefficient ($\boldsymbol{R^2}$) of Langmuir and Freundlich model are listed on **Table 3**, respectively. In this work, the value of $\boldsymbol{Q_m}$ and ***b*** from Langmuir model on CNT-PDA-PEI are 70.9 mg/g and 0.0511 L/mg, respectively. And $\boldsymbol{R^2}$ from Langmuir model is 0.991. As for Freundlich model, the value of $\boldsymbol{K_F}$ is 12.2 (mg/g) (L/mg) $^{1/n}$, ***n*** is 2.84, and $\boldsymbol{R^2}$ is 0.89 at 298 K.

As the result shown in **Table 3**, the Langmuir model gets higher value of correlation coefficient ($\boldsymbol{R^2}$) than Freundlich model, which represent the Langmuir isotherm model is more aligned with the experimental data then the Freundlich model. Additionally, the value of ***n*** (2.84) from Freundlich isotherm model means 1/***n*** is approximately equal to 0.35 between the numerical value of 0.1 to 0.5, which illustrate the favorable adsorption of $Cu^{2+}$ solution on CNT-PDA-PEI. According to all of above experimental data and computed results, we can conclude the consequence that active adsorption sites distribute homogeneously on the modified CNT-PDA-PEI nanocomposites, and the $Cu^{2+}$ removal process comply with the monolayer adsorption. Draw from the Langmuir model, the maximum amount of the adsorption capacity by modified CNT-PDA-PEI was reach to about 70.9 mg/g. Compared with the pristine CNTs and CNT-PDA, the results show the better adsorption efficiency on CNT-PDA-PEI for the removal of $Cu^{2+}$ solution from aqueous solution.

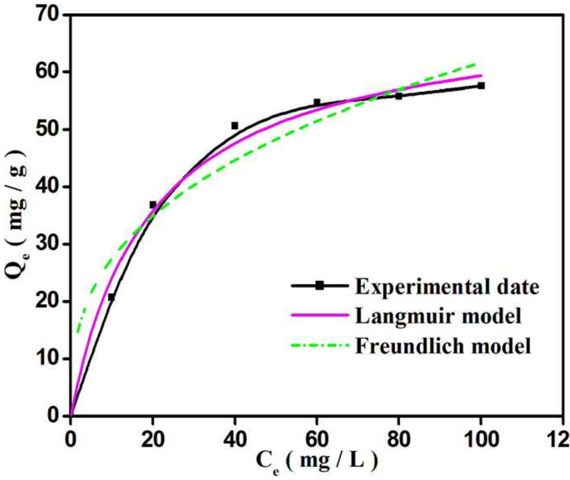

**Fig. 7** Adsorption isotherms of $Cu^{2+}$ on CNT-PDA-PEI. Experimental condition: adsorbent dose 10 mg, initial $Cu^{2+}$ concentrations from 10 mg/L to 100 mg/L. The value of data fitted by Langmuir model and Freundlich model, respectively.

**Table 3** Adsorption isotherms data of Langmuir and Freundlich model for $Cu^{2+}$ adsorption on CNT-PDA-PEI.

| Isotherms | Parameters | Temperatures (K) |
|---|---|---|
| | | 292 |
| Langmuir | $\boldsymbol{Q_0}$ (mg/g) | 70.9 |
| | ***b*** (L/mg) | 0.0511 |
| | $\boldsymbol{R^2}$ | 0.991 |
| Freundlich | $\boldsymbol{K_F}$ [(mg/g)(L/mg)$^{1/n}$] | 12.2 |
| | ***n*** | 2.84 |
| | $\mathbf{R^2}$ | 0.893 |

### 3.2.5 Effect of adsorbent dosage

As concluded from **Fig. 8**, increasing the adsorbent dosage resulted in an increase in the percentage removal of $Cu^{2+}$. Afterwards, with the continuous increase of the CNT-PDA-PEI, the removal percentage R (%) reached up to about 92% that got close to a hundred percent and remained steady. The adsorption capacity variation could be connected to the adsorbent concentration change, which may due to the variety of the modified adsorbent surface area and functional groups. Some ways for the practical adsorption application of these CNTs based adsorbents may be adopted. For example, we can fill these modified CNTs based adsorbents in column and the wastewater can be purified by these adsorbents filled column. On the other hand, these adsorbents can be conjugated with magnetic nanoparticles, and therefore these hybrid adsorbents can seperated from water using magnetic field.

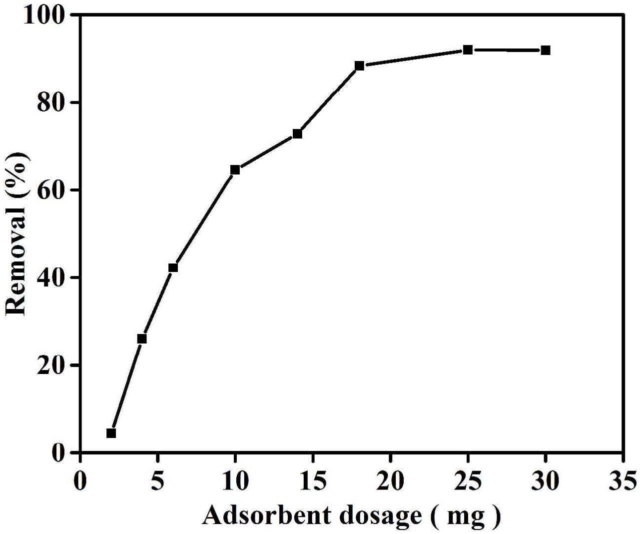

**Fig. 8** Effect of adsorbent dosage on removal of $Cu^{2+}$. Experimental conditions: reaction time: 120 min, $Cu^{2+}$ concentration: 10 mg/L, room temperature and neutral pH.

## Conclusion

In summary, a facile, efficient and rapid approach was reported for the preparation of an excellent absorbent with great dispersibility based on attractive CNTs for the removal of $Cu^{2+}$ from aqueous solution in this work via combination mussel-inspired chemistry and Michael addition reaction method. Characterized techniques including TEM, FT-IR and TGA were employed to ensure the successful surface modification of CNTs with PDA and PEI. With regard to the adsorption experiments, the effects of contact time, pH, temperature and initial concentrations were investigated. On the other hand, according to the adsorption experiments for $Cu^{2+}$ removal at different impacts (temperature, time, pH, $Cu^{2+}$ concentration), the adsorption capacity of CNT-PDA-PEI is increased along with the enhanced of time, pH and temperature, suggesting improved adsorption capability of CNTs modified with PEI. Furthermore, the positive value of ΔH° and the negative value of ΔG° indicated that the removal of $Cu^{2+}$ using CNT-PDA-PEI as adsorbents is endothermic and spontaneous. And the parameters for the Langmuir and Freundlich isotherms are calculated. The authentic purpose of this communication is aimed to provide a facile and versatile method for fabrication of high efficiency adsorbents, which should be of great importance for the environmental management.

## Acknowledgements

This research was supported by the National Science Foundation of China (Nos. 21134004, 21201108, 51363016, 21474057), and the National 973 Project (Nos. 2011CB935700).

## Notes

[a] Department of Environmental and Chemical Engineering, [b] Department of Chemistry and Jiangxi Provincial Key Laboratory of New Energy Chemistry, Nanchang University, 999 Xuefu Avenue, Nanchang 330031, China. [c] Department of Chemistry and the Tsinghua Center for Frontier Polymer Research, Tsinghua University, Beijing, 100084, P. R. China.

xiaoyongzhang1980@gmail.com; weiyen@tsinghua.edu.cn; lulong@ncu.edu.cn.

† Electronic Supplementary Information (ESI) available: [TEM images and TGA analysis of CNT samples were provided in supplementary information]. See DOI: 10.1039/b000000x/

## References

1. V. K. Gupta, I. Ali, T. A. Saleh, A. Nayak and S. Agarwal, *RSC Adv.*, 2014, **2**, 6380-6388.
2. A. Bhatnagar, F. Kaczala, W. Hogland, M. Marques, C. A. Paraskeva, V. G. Papadakis and M. Sillanpää, *Environ. Sci. Pollut. R.*, 2014, **21**, 268-298.
3. F. Fu and Q. Wang, *J. Environ. Manage.*, 2011, **92**, 407-418.
4. K. Rana, M. Shah and N. Limbachiya, *Int. J. Adv. Eng. Res. Sci.*, 2014, **1**, 55-59.
5. L. Ranjbar, Y. Yamini, A. Saleh, S. Seidi and M. Faraji, *Microchim. Acta.*, 2012, **177**, 119-127.
6. S. K. Das, I. Shome and A. K. Guha, *RSC Adv.*, 2012, **2**, 3000-3007.
7. K. Yang, W. Wei, L. Qi, W. Wu, Q. Jing and D. Lin, *RSC Adv.*, 2014, **4**, 46122-46125.
8. Y. Liu, M. Chen and H. Yongmei, *Chem. Eng. J.*, 2013, **218**, 46-54.
9. B. Murphy and B. Hathaway, *Coordin. Chem. Rev.*, 2003, **243**, 237-262.
10. M. Kazemipour, M. Ansari, S. Tajrobehkar, M. Majdzadeh and H. R. Kermani, *J. Hazard. Mater.*, 2008, **150**, 322-327.
11. H. A. Qdais and H. Moussa, *Desalination*, 2004, **164**, 105-110.
12. A. Dąbrowski, Z. Hubicki, P. Podkoscielny and E. Robens, *Chemosphere*, 2004, **56**, 91-106.
13. Y.-P. Zhu, Y.-L. Liu, T.-Z. Ren and Z.-Y. Yuan, *RSC Adv.*, 2014, **4**, 16018-16021.
14. S. Zhang, J. Li, T. Wen, J. Xu and X. Wang, *RSC Adv.*, 2013, **3**, 2754-2764.
15. S. Dib, M. Boufatit, S. Chelouaou, F. Sadi-Hassaine, J. Croissant, J. Long, L. Raehm, C. Charnay and J.-O. Durand, *RSC Adv.*, 2014, **4**, 24838-24841.
16. S. Yang, D. Shao, X. Wang and M. Nagatsu, *RSC Adv.*, 2014, **4**, 4856-4863.
17. B. Zou, K. Chen, Y. Wang, C. Niu and S. Zhou, *RSC Adv.*, 2015, **5**, 22973-22979.
18. S.-T. Yang, Y. Chang, H. Wang, G. Liu, S. Chen, Y. Wang, Y. Liu and A. Cao, *J. Colloid Interf. Sci.*, 2010, **351**, 122-127.
19. C. Cheng, S. Li, J. Zhao, X. Li, Z. Liu, L. Ma, X. Zhang, S. Sun and C. Zhao, *Chem.Eng. J.*, 2013, **228**, 468-481.
20. R. H. Baughman, A. A. Zakhidov and W. A. de Heer, *Science*, 2002, **297**, 787-792.
21. J. L. Gong, B. Wang, G. M. Zeng, C. P. Yang, C. G. Niu, Q. Y. Niu, W. J. Zhou and Y. Liang, *J. Hazard. Mater.*, 2009, **164**, 1517-1522.
22. S. A. Kosa, G. Al Zhrani and M. A. Salam, *Chem. Eng. J.*, 2012, **181**, 159-168.
23. Y. Li, F. Liu, B. Xia, Q. Du, P. Zhang, D. Wang, Z. Wang and Y. Xia, *J. Hazard. Mater.*, 2010, **177**, 876-880.
24. Y. H. Li, J. Ding, Z. Luan, Z. Di, Y. Zhu, C. Xu, D. Wu and B. Wei, *Carbon*, 2003, **41**, 2787-2792.
25. G. P. Rao, C. Lu and F. Su, *Sep. Purif. Technol.*, 2007, **58**, 224-231.
26. S. Rosenzweig, G. A. Sorial, E. Sahle-Demessie, D. C. McAvoy and A. A. Hassan, *Water, Air, & Soil Pollution*, 2014, **225**, 1-17.
27. E. Salehi, S. Madaeni, L. Rajabi, V. Vatanpour, A. Derakhshan, S. Zinadini, S. Ghorabi and H. A. Monfared, *Sep. Purif. Technol.*, 2012, **89**, 309-319.
28. A. Stafiej and K. Pyrzynska, *Sep. Purif. Technol.*, 2007, **58**, 49-52.
29. C. H. Wu, *J. Colloid Inter. Sci.*, 2007, **311**, 338-346.
30. C. Zhang, J. Sui, J. Li, Y. Tang and W. Cai, *Chem. Eng. J.*, 2012, **210**, 45-52.
31. G. Zhao, T. Wen, C. Chen and X. Wang, *RSC Adv.*, 2012, **2**, 9286-9303.
32. F. Gojny, M. Wichmann, U. Köpke, B. Fiedler and K. Schulte, *Compos.Sci. Technol.*, 2004, **64**, 2363-2371.
33. S. W. Kim, T. Kim, Y. S. Kim, H. S. Choi, H. J. Lim, S. J. Yang and C. R. Park, *Carbon*, 2012, **50**, 3-33.
34. P. Liu, *Eur. Polym. J.*, 2005, **41**, 2693-2703.
35. M. Gkikas, B. P. Das, M. Tsianou, H. Iatrou and G. Sakellariou, *Eur. Polym. J*, 2013, **49**, 3095-3103.
36. X. Zhang, K. Wang, M. Liu, X. Zhang, L. Tao, Y. Chen and Y. Wei, *Nanoscale*, 2015, **7**, 11486-11508.
37. Q. Wan, M. Liu, J. Tian, F. Deng, G. Zeng, Z. Li, K. Wang, Q. Zhang, X. Zhang and Y. Wei, *Polym. Chem.*, 2015, **6**, 1786-1792.
38. B. Yang, Y. Zhao, X. Ren, X. Zhang, C. Fu, Y. Zhang, Y. Wei and L. Tao, *Polym. Chem.*, 2015, **6**, 509-513.
39. X. Ren, B. Yang, Y. Zhao, X. Zhang, X. Wang, Y. Wei and L. Tao, *Polymer*, 2015, **64**, 210-215.
40. Y. Cao, X. Zhang, L. Tao, K. Li, Z. Xue, L. Feng and Y. Wei, *ACS Appl. Mater. Inter.*, 2013, **5**, 4438-4442.
41. J. Cui, Y. Yan, G. K. Such, K. Liang, C. J. Ochs, A. Postma and F. Caruso, *Biomacromolecules*, 2012, **13**, 2225-2228.
42. S. M. Kang, S. Park, D. Kim, S. Y. Park, R. S. Ruoff and H. Lee, *Adv Funct Mater.*, 2011, **21**, 108-112.
43. H. Lee, S. M. Dellatore, W. M. Miller and P. B. Messersmith, *Science*, 2007, **318**, 426-430.
44. J. Wu, L. Zhang, Y. Wang, Y. Long, H. Gao, X. Zhang, N. Zhao, Y. Cai and J. Xu, *Langmuir*, 2011, **27**, 13684-13691.
45. S. H. Yang, S. M. Kang, K. B. Lee, T. D. Chung, H. Lee and I. S. Choi, *J. Am. Chem. Soc.*, 2011, **133**, 2795-2797.
46. Q. Zhu and Q. Pan, *ACS Nano*, 2014, **8**, 1402-1409.
47. H. Gao, Y. Sun, J. Zhou, R. Xu and H. Duan, *ACS Appl. Mater. Inter.*, 2013, **5**, 425-432.
48. Y. Liu, K. Ai and L. Lu, *Chem. Rev.*, 2014, **114**, 5057-5115.
49. Q. Ye, F. Zhou and W. Liu, *Chem. Soc. Rev.*, 2011, **40**, 4244-4258.
50. C. Cheng, S. Nie, S. Li, H. Peng, H. Yang, L. Ma, S. Sun and C. Zhao, *J. Mater. Chem. B*, 2013, **1**, 265-275.
51. C. Cheng, S. Sun and C. Zhao, *J. Mater. Chem. B*, 2014, **2**, 7649-7672.
52. H. Hu, B. Yu, Q. Ye, Y. Gu and F. Zhou, *Carbon*, 2010, **48**, 2347-2353.

53. Q. Wan, J. Tian, M. Liu, G. Zeng, Q. Huang, K. Wang, Q. Zhang, F. Deng, X. Zhang and Y. Wei, *Appl. Surf. Sci.*, 2015, **346**, 335-341.
54. X. Zhang, Q. Huang, M. Liu, J. Tian, G. Zeng, Z. Li, K. Wang, Q. Zhang, Q. Wan and F. Deng, *Appl. Surf. Sci.*, 2015, **343**, 19-27.
55. X. Zhang, G. Zeng, J. Tian, Q. Wan, Q. Huang, K. Wang, Q. Zhang, M. Liu, F. Deng and Y. Wei, *Appl. Surf. Sci.*, 2015, **351**, 425-432.
56. X. Zhang, S. Wang, L. Xu, L. Feng, Y. Ji, L. Tao, S. Li and Y. Wei, *Nanoscale*, 2012, **4**, 5581-5584.
57. M. Liu, J. Ji, X. Zhang, X. Zhang, B. Yang, F. Deng, Z. Li, K. Wang, Y. Yang and y. wei, *J. Mater. Chem. B*, 2015, **3**, 3476 - 3482.
58. X. Zhang, M. Liu, Y. Zhang, B. Yang, Y. Ji, L. Feng, L. Tao, S. Li and Y. Wei, *RSC Adv.*, 2012, **2**, 12153-12155.
59. X. Zhang, J. Ji, X. Zhang, B. Yang, M. Liu, W. Liu, L. Tao, Y. Chen and Y. Wei, *RSC Adv.*, 2013, **3**, 21817-21823.
60. Q. Wan, M. Liu, J. Tian, F. Deng, Y. Dai, K. Wang, Z. Li, Q. Zhang, X. Zhang and Y. Wei, *RSC Adv.*, 2015, **5**, 38316-38323.
61. Q. Wan, J. Tian, M. Liu, G. Zeng, Z. Li, K. Wang, Q. Zhang, F. Deng, X. Zhang and Y. Wei, *RSC Adv.*, 2015, **5**, 25329-25336.
62. M. Sun, B. Ding and J. Yu, *RSC Adv.*, 2013, **2**, 1373-1378.
63. S. Yang, J. Li, D. Shao, J. Hu and X. Wang, *J. Hazard. Mater.*, 2009, **166**, 109-116.